CHAPTER IV
RESULTS AND DISCUSSION

In the previous work, Jantawasu (2008) studied the photocatalytic degradation of Methyl Orange monoazo dye by comparatively using nanocrystalline mesoporous-assembled TiO$_2$ and non-mesoporous-assembled TiO$_2$ photocatalysts. The results showed that the synthesized mesoporous-assembled TiO$_2$ calcined at 500°C gave the highest efficiency in the Methyl Orange degradation. In this research, experimental investigation was performed on the photocatalytic degradation of a mixture of two azo dyes: monoazo Acid Yellow 23 (AY) containing 1 azo group and diazo Acid Black 1 (AB) containing 2 azo groups, as model contaminants in textile wastewater, using the mesoporous-assembled TiO$_2$ nanocrystal synthesized by the sol-gel process with the aid of the structure-directing surfactant and calcined at 500°C.

4.1 Characterization Results of TiO$_2$ Photocatalyst

4.1.1 N$_2$ Adsorption-Desorption Analysis

In order to verify the mesoporosity of the TiO$_2$ photocatalyst sample, N$_2$ adsorption-desorption analysis is very powerful technique normally used. The N$_2$ adsorption-desorption isotherms of the synthesized TiO$_2$ calcined at 500°C exhibits typical IUPAC type IV pattern (Rouquerol *et al.*, 1999), as shown in Figure 4.1(a). The hysteresis loop is ascribed to the existence of mesoporous structure (mesopore size between 2 and 50 nm) in the obtained product. A sharp increase in adsorption volume of N$_2$ was observed and located in the P/P$_0$ range of 0.5-0.9. This sharp increase can be assigned to the capillary condensation of N$_2$ into the pores, indicating good homogeneity of the sample and fairly small pore size since the P/P$_0$ position of the inflection point is directly related to pore dimension. As illustrated in Figure 4.1(b), the pore size distribution obtained from this modified sol-gel process is quite narrow and monomodal, also implying good quality of the sample. For the textural properties of the investigated photocatalyst, its BET surface area, mean pore diameter, and total pore volume are 84.3 m^2/g, 6.18 nm, and 0.16 cm^3/g, respectively.
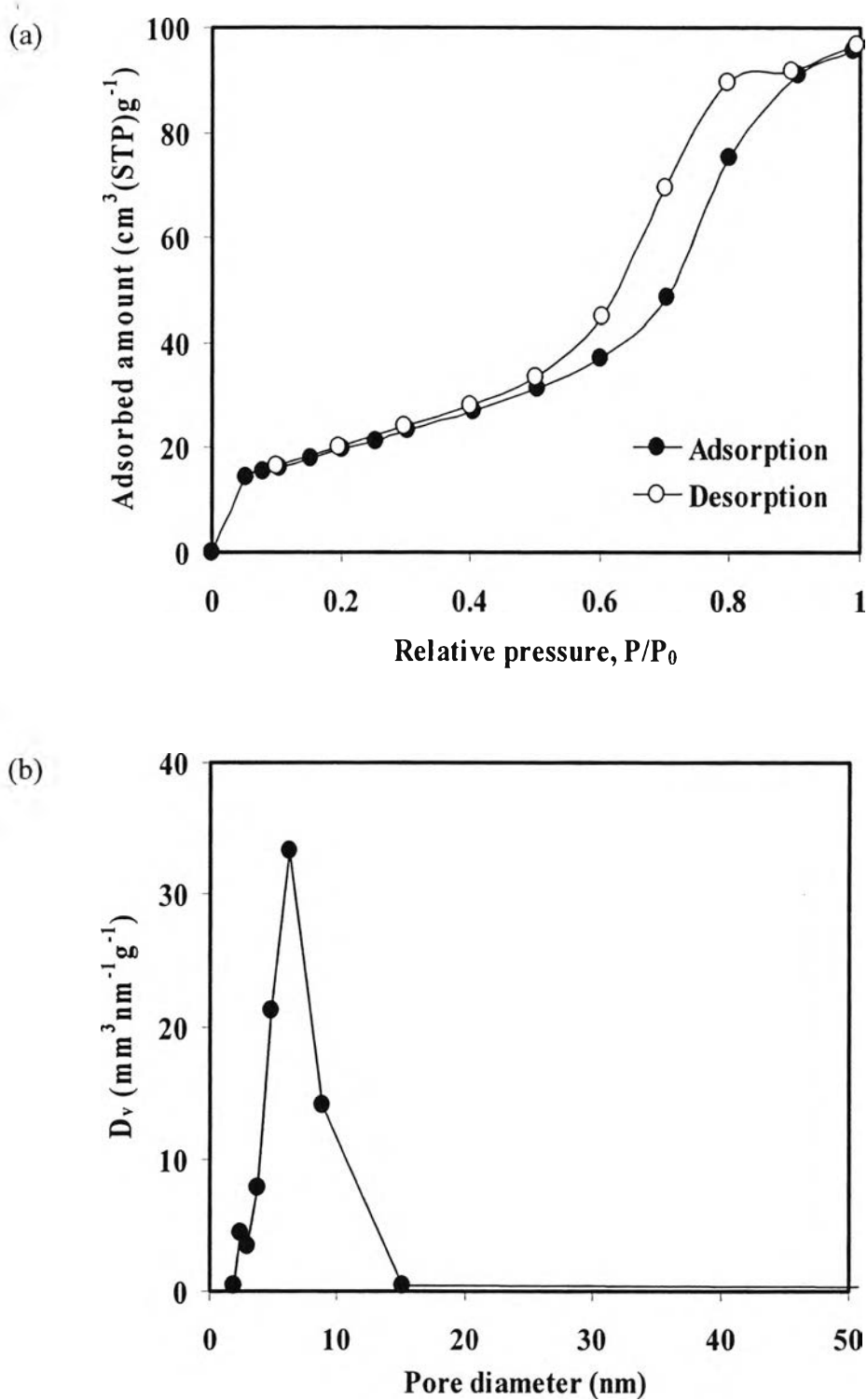
(a)

(b)

Figure 4.1 (a) N_2 adsorption–desorption isotherms and (b) pore size distribution of the synthesized mesoporous-assembled TiO_2 calcined at 500°C.

4.1.2 X-ray Diffraction Analysis

The XRD pattern of the synthesized mesoporous-assembled TiO_2 photocatalyst is shown in Figure 4.2. The XRD pattern shows crystalline structure of the pure anatase phase. The dominant peaks at 2θ about 25.2, 37.9, 47.8, 53.8, and 55.0°, which represent the indices of (101), (004), (200), (105), and (211) planes (JCPDS Card No. 21-1272) (Smith, 1960), respectively, are conformed to crystalline structure of the anatase TiO_2. The crystallite size of the investigated photocatalyst estimated from the line broadening of the anatase (101) diffraction peak by the Sherrer equation (Cullity, 1978) is 13.64 nm.
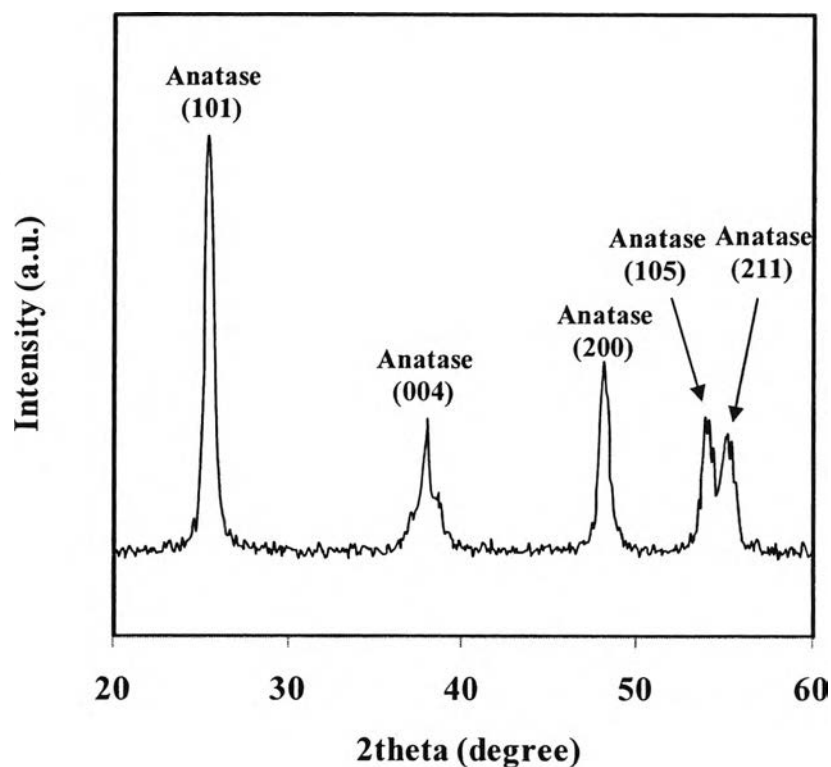

Figure 4.2 XRD pattern of the synthesized mesoporous-assembled TiO_2 calcined at 500°C.

4.1.3 UV-Visible Spectroscopy

UV-Visible spectroscopy was used to investigate the light absorption capability of the photocatalyst. The UV-Vis spectrum of the synthesized mesoporous-assembled TiO_2 photocatalyst is shown in Figure 4.3.
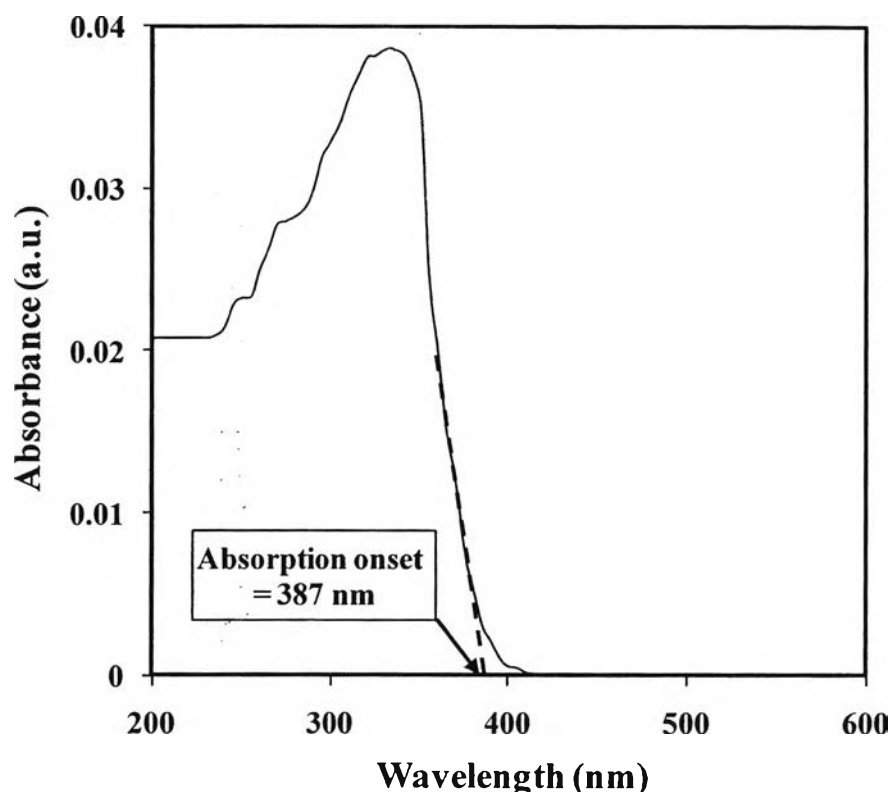

Figure 4.3 UV -Visible spectrum of the synthesized mesoporous-assembled TiO_2 photocatalyst calcined at 500°C.

It can be clearly seen that, the absorption band of the TiO_2 photocatalyst is approximately in the range of 200-400 nm. The strong absorption band at low wavelength in the spectrum indicated the presence of Ti species as tetrahedral Ti^{4+}. This absorption band is generally associated with the electronic excitation of the valence band O2p electron to the conduction band Ti3d level (Fuerte *et al.*, 2002). The absorption onset of the synthesized mesoporous-assembled TiO_2 is approximately at 387 nm, which corresponds to the band gap energy of the anatase TiO_2 of 3.2 eV.

4.1.4 TEM Analysis

Typical TEM images (for both low and high magnifications) of the investigated photocatalyst are shown in Figure 4.4. The low-magnification TEM image demonstrates the formation of TiO_2 aggregates composed of three-dimensional disordered primary nanoparticles, where the high-magnification TEM image reveals the high crystallinity of the photocatalyst. The average particle size of the mesoporous-assembled TiO_2 nanoparticles calcined at 500°C is approximately 10-15 nm, which is consistent with the crystallite size estimated from the XRD analysis. Therefore, each nanoparticle observed by the TEM analysis could be plausibly considered as a single crystal.
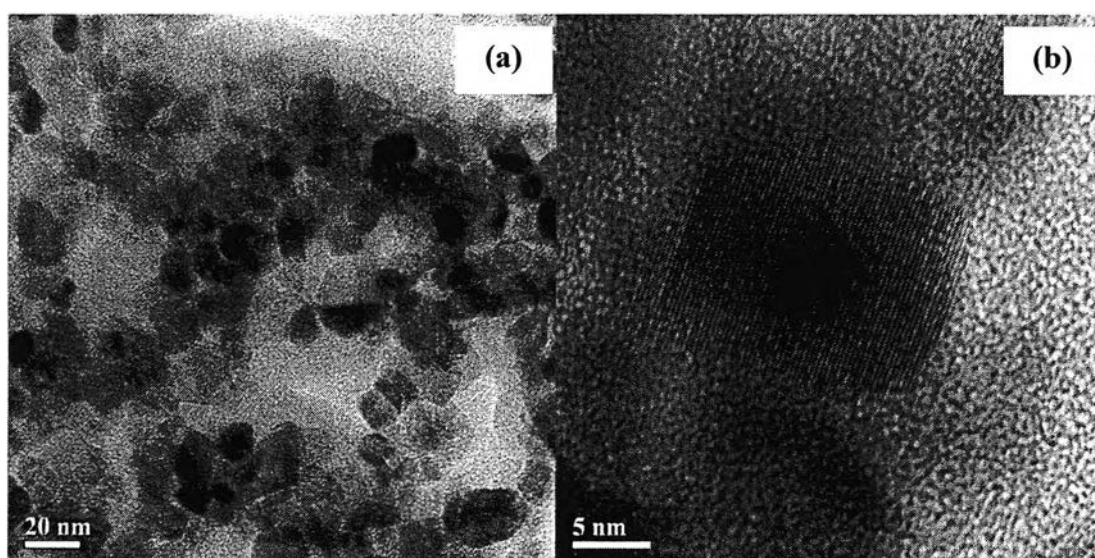

Figure 4.4 TEM images of the synthesized mesoporous-assembled TiO_2 calcined at 500°C: (a) low magnification and (b) high magnification.

4.1.5 Point of Zero Charge (PZC)

The point of zero charge (PZC) is a very important parameter used to determine the surface charge property of the photocatalyst under a particular environment. The point of zero charge is defined as the pH, at which the surface charge of the photocatalyst is neutral, i.e. the number of positive charges on the surface being equal to that of negative charges. Figure 4.5 shows the correlation between initial pH and final pH at equilibrium of the aqueous solution suspended with the synthesized mesoporous-assembled TiO_2. For the investigated TiO_2 photocatalyst, it could be experimentally observed that its PZC is approximately 5.8, which is similar to the reported value of 6.0 ± 0.3 for TiO_2 in the literature (Parks, 1965).
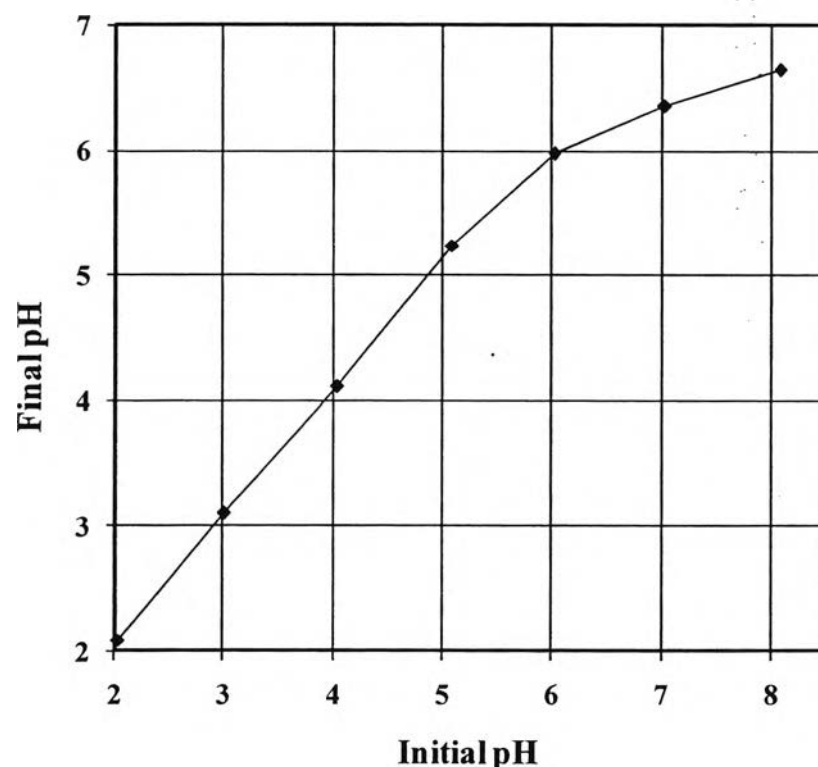

Figure 4.5 Correlation between initial pH and final pH at equilibrium of the aqueous solution suspended with the synthesized mesoporous-assembled TiO_2 calcined at 500°C.

4.2 Photocatalytic AY and AB Degradation Results

4.2.1 UV-Visible Spectroscopy

UV-Visible spectroscopy was used to investigate the effects of various reaction parameters on the degradation of single and mixed dyes. The UV-Visible spectra of AY and AB measured separately are shown in Figure 4.6. They reveal the λ_{max} values of AY and AB at 425 and 619 nm, respectively. For the mixture of AY and AB, it is evident that the λ_{max} values of both dyes did not change upon the mixing at different irradiation times during the course of photocatalytic degradation using the mesoporous-assembled TiO_2 photocatalyst, as shown in Figure 4.7. This indicates that the decreases in their λ_{max} values could be used to evaluate the degradation performance for each dye separately. Gupta *et al.* (2006) also explained that the photocatalytic degradation of the mixture of Crystal Violet and Methyl Red dyes could be studied separately by using their corresponding λ_{max} values of 590 and 430 nm, respectively.
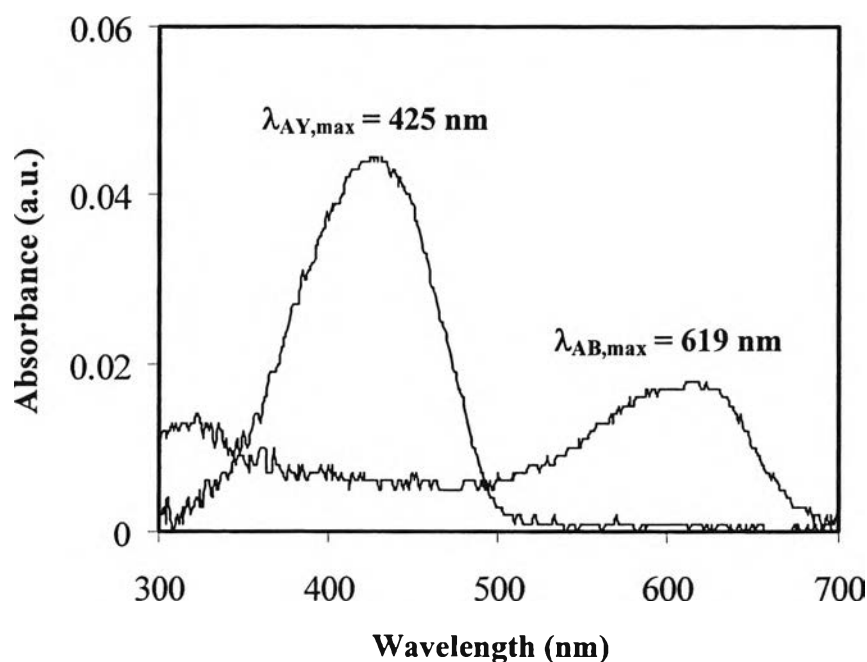

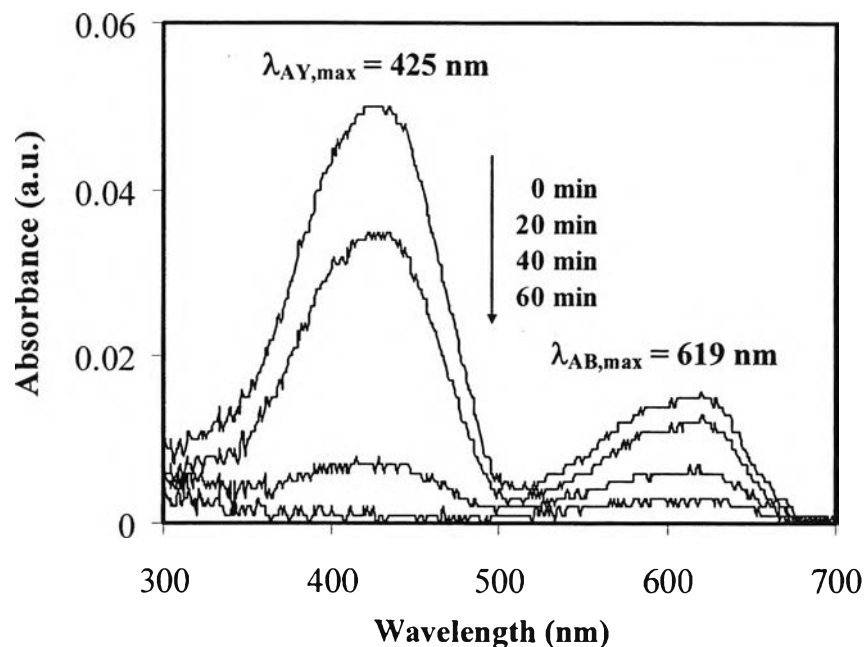**Figure 4.6** UV-Visible spectra of AY and AB measured separately.

Figure 4.7 UV-Visible spectra of a mixture of AY and AB as a function of irradiation time during their photocatalytic degradation using the synthesized mesoporous-assembled TiO_2 photocatalyst.

4.2.2 Effect of Initial Dye Concentration

Six groups of dye solutions prepared by mixing AY and AB at different concentration ratios were used to study the effect of initial dye concentration on the photocatalytic degradation performance to find their suitable mixing ratio by using the synthesized mesoporous-assembled TiO_2 photocatalyst. The investigated ranges of initial AY and AB concentrations for the mixtures are shown in Table 4.1. There are 2 sets of photocatalytic experiment: one with constant initial AY concentrations at 2.5, 5 and 10 mg/l and various initial AB concentrations in the range of 0 to 10 mg/l (Mix I, Mix II, and Mix III), and the other with constant initial AB concentrations at 2.5, 5 and 10 mg/l and various initial AY concentrations in the range of 0 to 10 mg/l (Mix IV, Mix V, and Mix VI). The mixtures with total volume of 80 ml containing 5 g/l of the mesoporous-assembled TiO_2 were initially used for the photocatalytic activity testing. The degradation rate constants (k) at various initial dye concentrations are shown in Figure 4.8(a) for constant initial AY concentrations and Figure 4.8(b) for constant initial AB concentrations. It can be

observed that at any given initial AY and AB concentrations, the degradation rate constant of AY is always higher than that of AB, indicating that AY could be more easily degraded by the TiO_2 photocatalyst. This is possibly because AY is a monoazo dye with less molecular complexity than AB, which is a diazo dye, resulting in an easier attack of AY dye by several photogenerated active species. When maintaining initial concentration of AY or AB at 2.5, 5 and 10 mg/l and increasing initial concentration of the other, the degradation rate constants of both dyes reached the maximum at the other dye concentration of 2.5 mg/l and then gradually decreased possibly due to too large number of dye molecules to be attacked by the active species.

It is interestingly found that when maintaining initial AB concentration constant and varying initial AY concentration (Figure 4.8(b)), the degradation rate constants of both dyes tended to be higher than those when maintaining initial AY concentration constant and varying initial AB concentration (Figure 4.8(a)), especially at initial AY and AB concentrations of 2.5 and 5 mg/l, respectively, for Mix V. Since a mixture of 5 mg/l AY and 2.5 mg/l AB and a mixture of 2.5 mg/l AY and 5 mg/l AB provided the highest photocatalytic efficiency in each experimental set, these two mixtures were used in further experiments to optimize the reaction parameters.

Table 4.1 Various conditions of initial dye concentration of AY and AB used for photocatalytic activity testing

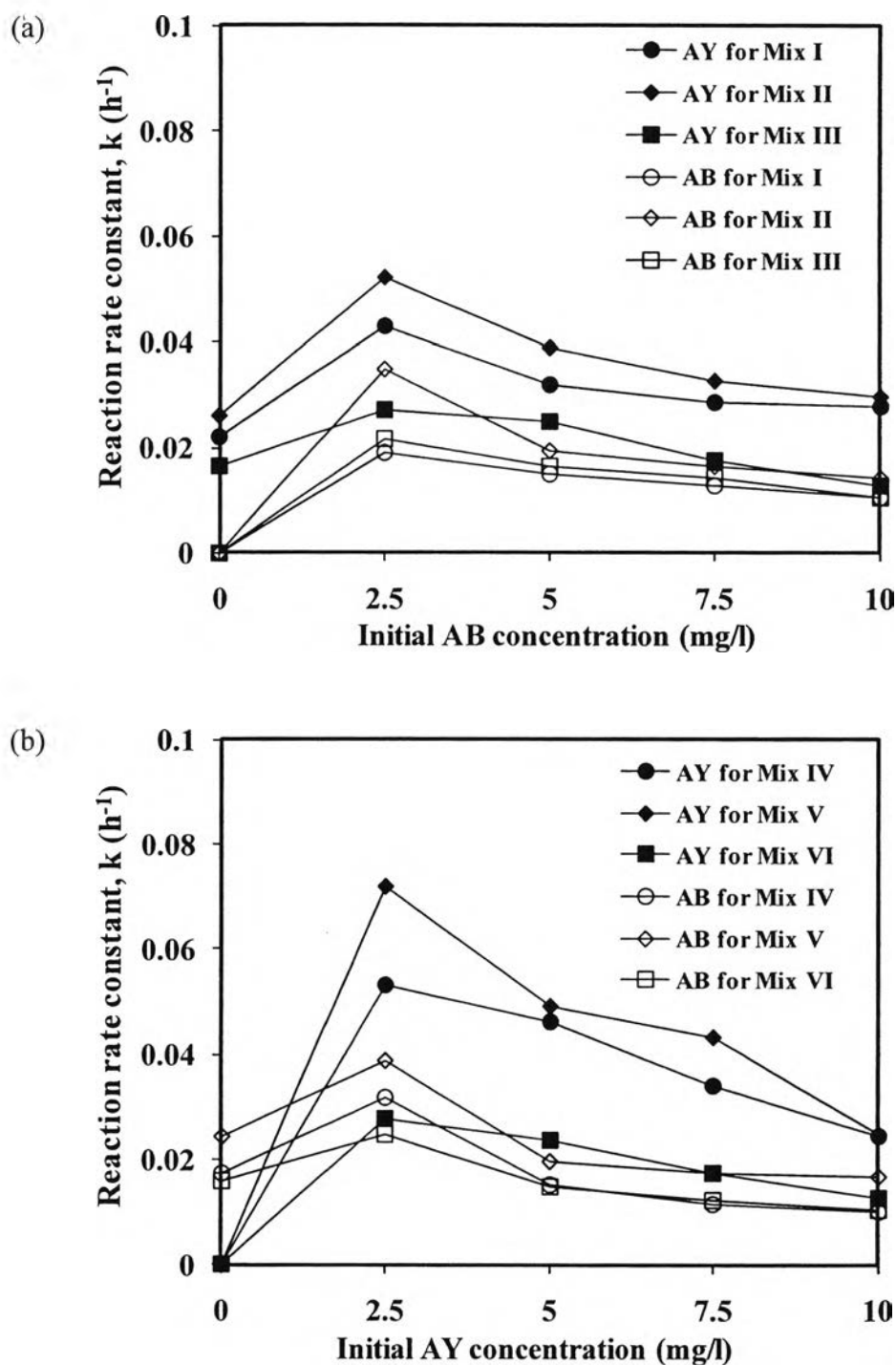| Mixture	Initial dye concentration (mg/l)	
	AY	AB
Mix I	2.5	0-10
Mix II	5	0-10
Mix III	10	0-10
Mix IV	0-10	2.5
Mix V	0-10	5
Mix VI	0-10	10

Figure 4.8 Effect of initial dye concentration on degradation rate constant for (a) constant AY concentrations at 2.5, 5, and 10 mg/l and various AB concentrations (b) constant AB concentrations at 2.5, 5, and 10 mg/l and various AY concentrations using the synthesized mesoporous-assembled TiO_2 photocatalyst (photocatalyst dosage = 5 g/l, reaction volume = 80 ml, irradiation time = 2 h).

4.2.3 Effect of Photocatalyst Dosage

The effect of photocatalyst dosage on the photocatalytic degradation of the mixtures of AY and AB was next investigated. The results of photocatalytic degradation using various photocatalyst dosages of the synthesized mesoporous-assembled TiO_2 are shown in Figure 4.9(a) for AY and AB concentrations of 5 and 2.5 mg/l, respectively, and in Figure 4.9(b) for AY and AB concentrations of 2.5 and 5 mg/l, respectively. In the case of the photolysis (reaction in the absence of the photocatalyst), the degradation efficiency was very comparatively low, therefore the photocatalyst was necessary for the photocatalytic reaction. The results indicate that significant increases in the photocatalytic degradation efficiency were observed when the photocatalyst dosage was increased to 10 g/l. However, when it exceeded 10 g/l, the photocatalytic degradation efficiency adversely decreased. The photocatalytic degradation efficiencies at this optimum photocatalyst dosage value of 10 g/l for the mesoporous-assembled TiO_2 nanoparticle were 99.1% for AY and 95.7% for AB of the mixture of 2.5 mg/l AY and 5 mg/l AB, and 98% for AY and 94.2% for AB of the mixture of 5 mg/l AY and 2.5 mg/l AB. The TOC results also showed similar degradation efficiency to that determined by the UV-Visible spectroscopy. The maximum TOC removal for the mixture of 2.5 mg/l AY and 5 mg/l AB was 92.5%, which was higher than that for the mixture of 5 mg/l AY and 2.5 mg/l AB of 91.3%.
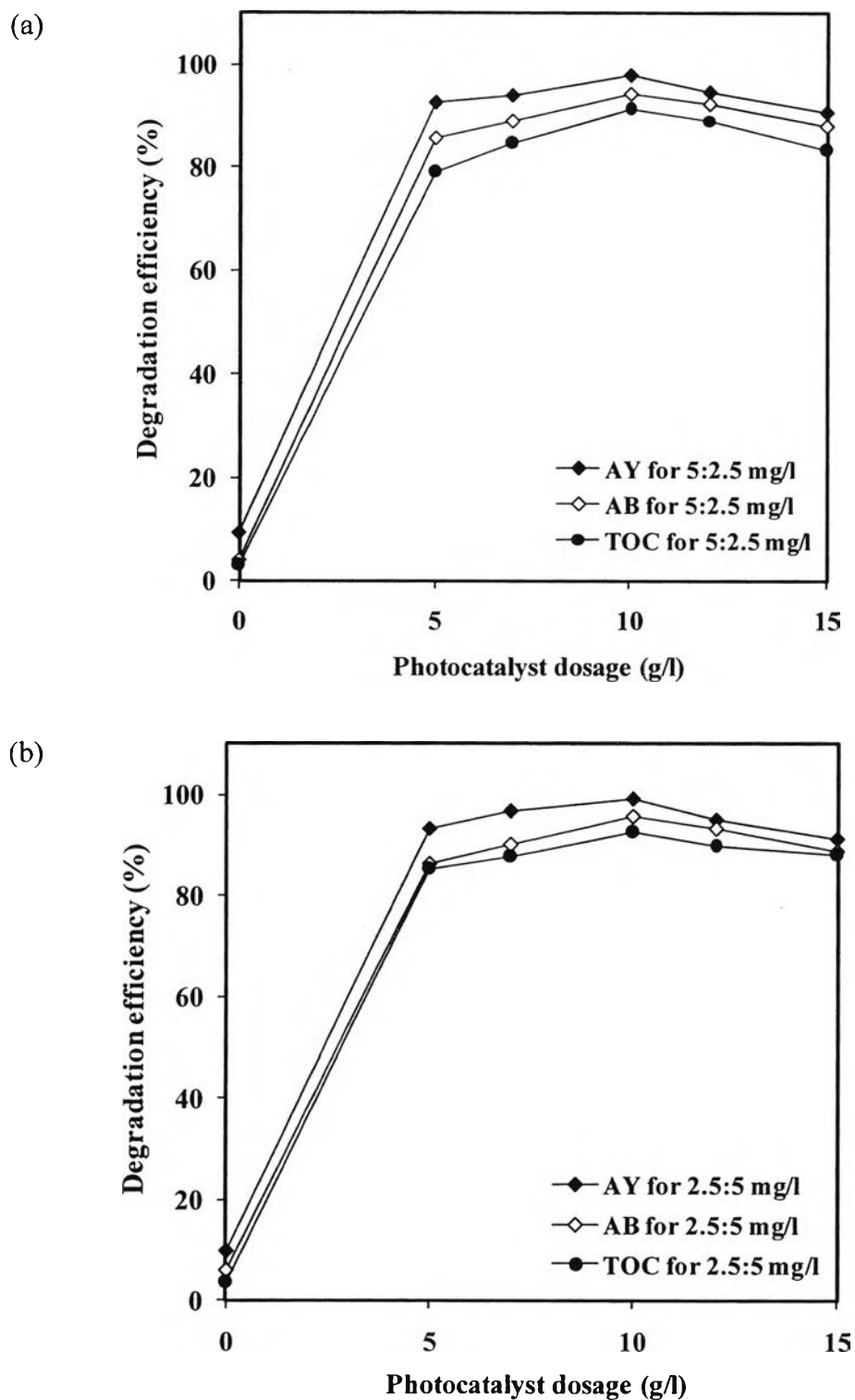
(a)

(b)

Figure 4.9 Effect of photocatalyst dosage on degradation efficiency for (a) mixture of AY 5 mg/l and AB 2.5 mg/l and (b) mixture of AY 2.5 mg/l and AB 5 mg/l using the synthesized mesoporous-assembled TiO_2 photocatalyst (reaction volume = 80 ml, irradiation time = 90 min).

On the basis of the relevant band gap absorption of the investigated photocatalyst dosage, the results can be explained in terms of the availability of active sites on the TiO_2 surfaces, the light absorption ability, and the light penetration depths into the suspension. With increasing the photocatalyst dosage until reaching the optimum value, the TiO_2 surface active sites, as well as the light absorption ability of the TiO_2, accordingly increase. On the other hand, at higher photocatalyst dosage, there is only a small portion of productive particles near the photocatalytic reactor wall that can completely absorb the incident light. The photocatalyst also has high tendency to be agglomerated, and therefore low amount of the photocatalyst can absorb the irradiating light. Furthermore, the light penetration depths become less due to the agglomeration and sedimentation of particles under a higher photocatalyst dosage, which could result in the light scattering and shielding, thus dramatically reducing the intensity of light entering the irradiated suspension (Konstantinou and Albanis, 2004).

4.2.4 Effect of Dissolved Oxygen

The effect of dissolved oxygen on the photocatalytic degradation of the mixtures of AY and AB was further investigated. The photocatalytic degradation experiments were carried out under the bubbling of different gases into the suspension. The dissolved oxygens in the case of N_2, Air, and O_2 bubblings were 0, 8.8, and 37.7 mg/l, respectively (Chavadej et al., 2008), as compared to 7.5 mg/l of the naturally dissolved oxygen in water in the case of no gas bubbling (Boyd, 2004). The results of degradation efficiency of the mixtures of AY and AB at various dissolved oxygens are depicted in Figures 4.10(a) and (b). It can be noticed that the O_2 facilitates the degradation efficiency of both AY and AB. When the TiO_2 particles are irradiated by photons with appropriate energy, the valence band electrons of the TiO_2 can be excited to the condition band, creating highly reactive electron (e^-) and hole (h^+) pairs. These photogenerated species migrate to the TiO_2 solid surface and are trapped at different sites. These electrons and holes play a part in the reduction and oxidation of the photocatalytic reaction, respectively. The photogenerated holes can be trapped by hydroxyl ions on the photocatalyst surface to form active hydroxyl radicals, and the electrons can be additionally trapped by oxygen, as an electron

acceptor, from both air and pure O_2 bubblings to form active oxygen species (O_2^-) on the photocatalyst surface (Kim *et al.*, 2002). Thus, the photocatalytic degradation can be increased due to the formation of the active oxygen species. As previously stated, while the oxygen can act as an electron acceptor to form active oxygen species, the nitrogen cannot act in such a manner, resulting in a lower photocatalytic degradation efficiency in the case of N_2 bubbling, which eliminated all dissolved oxygen molecules from the suspension. Even though the air and O_2 bubblings could enhance the photocatalytic degradation efficiency, the originally dissolved oxygen in the case of no gas bubbling seemed to be sufficient to obtain comparatively high photocatalytic efficiency. Therefore, the gas bubbling was not required for further experiments.
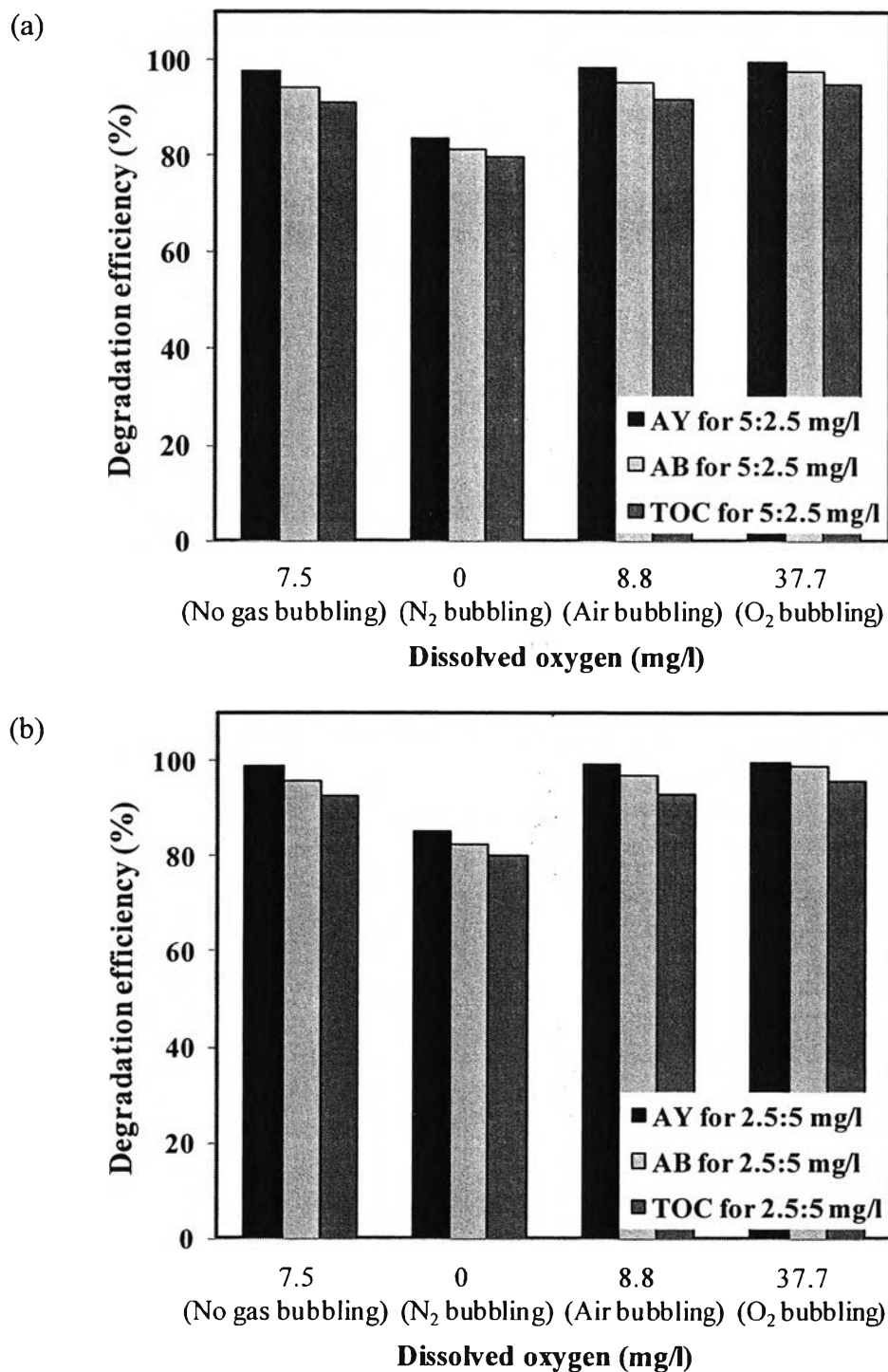
Figure 4.10 Effect of dissolved oxygen on degradation efficiency for (a) mixture of AY 5 mg/l and AB 2.5 mg/l and (b) mixture of AY 2.5 mg/l and AB 5 mg/l using the synthesized mesoporous-assembled TiO_2 photocatalyst (photocatalyst dosage = 10 g/l, reaction volume = 80 ml, irradiation time = 90 min).

4.2.5 Effect of Initial Solution pH

The wastewaters in the environment usually have a wide range of pH values. Commonly, the pH of solution is an important parameter in the photocatalytic processes, since it not only plays an important role on the characteristics of wastewaters but also determines the surface charge properties of TiO_2, the size of aggregates formed, the charge of dye molecules, the adsorption of dyes onto TiO_2 surface, and the concentration of hydroxyl radicals. In this work, both the mixture of 5 mg/l AY and 2.5 mg/l AB and the mixture of 2.5 mg/l AY and 5 mg/l AB were subjected to the photocatalytic degradation in the initial solution pH range of 4 to 7. The pH of the solution was adjusted by adding HCl and NaOH. Figures 4.11(a) and (b) show the degradation efficiency of the two mixtures over the synthesized mesoporous-assembled TiO_2 at various initial solution pHs.

When AY and AB dyes are dissolved in water, their structures become negatively charged. However, the TiO_2 surface is presumably positively charged when the initial solution pH is lower than its point of zero charge (PZC), which was experimentally found to be 5.8 (Figure 4.5). These opposite charges favorably lead to the enhancement of the photocatalytic degradation due to their increased interaction. The results indicate that the higher photocatalytic degradation occurred at pH lower than the PZC. The optimum pH value for this photocatalytic reaction system was found at an initial solution pH of 4.5. However, a further decrease in the initial solution pH from 4.5 to 4 led to a decrease in the degradation efficiency due to the plausible agglomeration of TiO_2 particles (Sun *et al.*, 2007), which consequently reduced the surface area available for both reactant adsorption and the photon absorption.
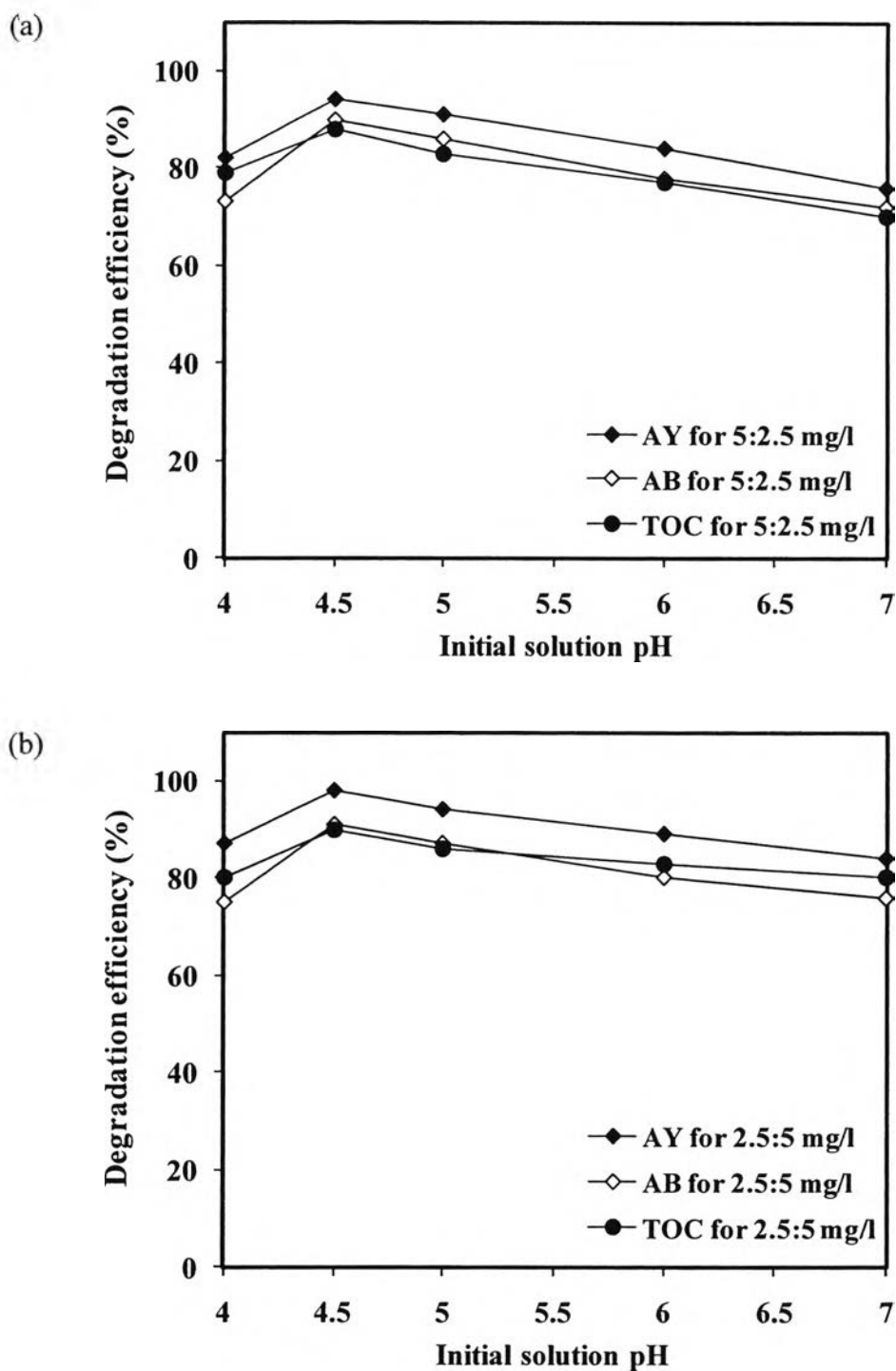
Figure 4.11 Effect of initial solution pH on degradation efficiency for (a) mixture of AY 5 mg/l and AB 2.5 mg/l and (b) mixture of AY 2.5 mg/l and AB 5 mg/l using the synthesized mesoporous-assembled TiO_2 photocatalyst (photocatalyst dosage = 10 g/l, reaction volume = 80 ml, irradiation time = 60 min).

Moreover, at too low pH with the excess concentration of H^+, the H^+ ions tend to interact with the azo link (–N=N–), at which, in turn, can preferentially be electrophilically attacked by hydroxyl radicals, leading to decreasing the electron densities at the azo group. Consequently, the reactivity of hydroxyl radicals by electrophilic mechanism decreases (Sun *et al.*, 2007). The decrease in the degradation efficiency at higher pHs than the PZC may be because the AY and AB are anionic dyes, and at high pH their negative charge are more pronounced. Hence, there may be a strong coulombic repulsion between the negatively charged surface of photocatalyst and the negatively charged AY and AB molecules (Konstantinou and Albanis, 2004), resulting in less adsorption probability of the dye molecules on the photocatalyst surface for the photocatalytic reaction.

4.2.6 Effect of Water Hardness

The presence of water hardness, as a part of natural organic matters, has been a problem in the many industries due to their water-soluble property and non-biodegradability. Hardness is generally referred to calcium and magnesium present in water with a typical Ca-to-Mg ratio of 3:2, and the normal total hardness concentration is about 120-240 mg/l (Tanthakit *et al.*, 2009). In this photocatalytic degradation study, the experiments were divided into 2 sets. For the first experimental set, different types and concentrations of water hardness, i.e. pure Ca, pure Mg, and mixture of Ca and Mg, were investigated with different total concentrations of 100, 200, and 500 mg/l for each case. The hardness concentration of 500 mg/l was used in the experiment to represent the extremely hard water. The experimental results are illustrated in Figures 4.12(a) and (b). The results indicate that the degradation efficiency tends to decrease with increasing hardness concentration. However, at the same total hardness concentration, Mg more negatively affected to the photocatalytic degradation efficiency than Ca. However, a mixture of Ca and Mg showed the worst effect to the photocatalytic degradation efficiency.

For the second set of the experiments, the total hardness concentration of 500 mg/l for the mixture of Ca and Mg, which led to the lowest photocatalytic degradation efficiency in the first experimental set, was chosen to further enhance the

efficiency by the pH adjustment. Seven tests were conducted with the same initial hardness concentration of mixed Ca and Mg of 500 mg/l at different initial solution pHs. The experimental results shown in Figure 4.13(a) and (b) reveal that the degradation efficiency decreased with increasing initial solution pH from 5 to 7. At an initial solution pH of 5.0, the maximum degradation efficiency of 92.5% for AY of the mixture of 2.5 mg/l AY and 5 mg/l AB could be obtained, being much closer to the degradation efficiency of the dye in water without hardness of 98% at an initial solution pH of 4.5. This may indicate that the adsorption of dye molecules played a significant role on the photocatalytic degradation, since the photocatalytic reaction mainly occurred on the surface of catalyst, but not in the bulk solution (Li *et al.*, 2002). However, at a lower initial solution pH of 4, the photocatalytic degradation efficiency decreased due to the plausible agglomeration of TiO_2 particles.

It could be observed that in case of the solution without hardness, the optimum pH was 4.5, which was lower than the optimum pH of 5 in the case of solution with hardness. In the experiments, the TiO_2 surface was positively charged since the solution pH was lower than the photocatalyst PZC. When the hardness was present in the solution, the positive charge in the solution was dramatically increased due to the positive cations of hardness, resulting in repulsion forces between the positive charges. This led to an obstruction of the dye molecules to adsorb on the TiO_2 surface. Particularly, the Mg cations could approach to TiO_2 surface easier than the Ca cations due to a smaller ionic radius, which made the dye adsorb more difficult. When the pH of the solution was increased to 5, the overall positive charge was decreased to achieve the well-balanced condition between the dye adsorption and the repulsion forces of the positive charges.
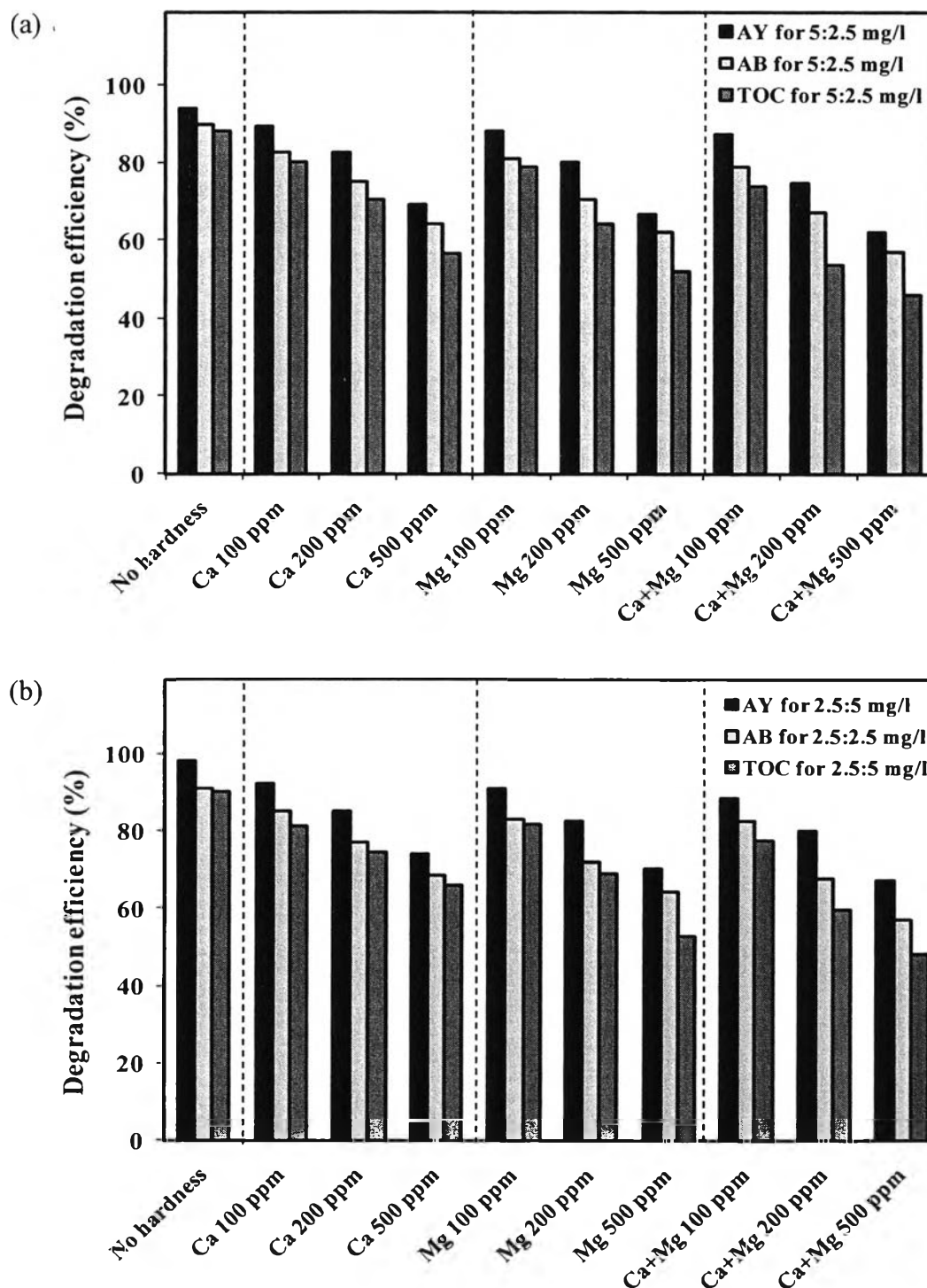
Figure 4.12 Effect of hardness type and concentration on degradation efficiency for (a) mixture of AY 5 mg/l and AB 2.5 mg/l and (b) mixture of AY 2.5 mg/l and AB 5 mg/l using the synthesized mesoporous-assembled TiO_2 photocatalyst (photocatalyst dosage = 10 g/l, reaction volume = 80 ml, irradiation time = 60 min, initial solution pH = 4.5).
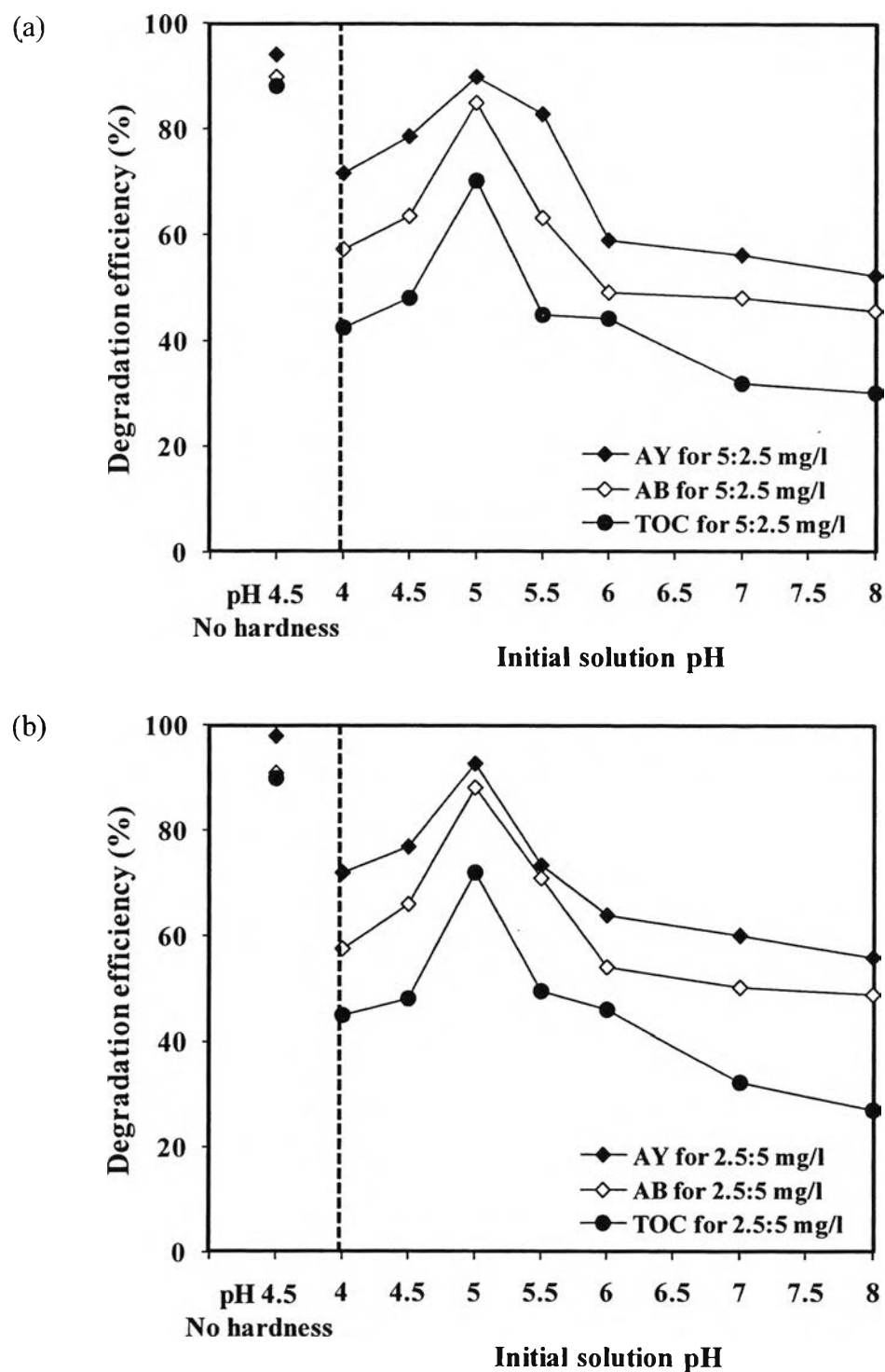
(a)

(b)

Figure 4.13 Effect of initial solution pH on degradation efficiency in the presence of hardness for (a) mixture of AY 5 mg/l and AB 2.5 mg/l and (b) mixture of AY 2.5 mg/l and AB 5 mg/l using the synthesized mesoporous-assembled TiO_2 photocatalyst (photocatalyst dosage = 10 g/l, reaction volume = 80 ml, irradiation time = 60 min, total hardness concentration = 500 mg/l).